

Reductive Half-Reaction of Thioredoxin Reductase from *Escherichia coli*<sup>†</sup>

Brett W. Lennon and Charles H. Williams, Jr.\*

Department of Biological Chemistry, University of Michigan, and Department of Veterans Affairs Medical Center, Ann Arbor, Michigan 48105

Received February 10, 1997; Revised Manuscript Received May 23, 1997<sup>®</sup>

**ABSTRACT:** Thioredoxin reductase is a homodimeric flavoenzyme containing a flavin adenine dinucleotide (FAD) and a redox-active disulfide in each subunit. Structural work on the enzyme from *Escherichia coli* suggests that thioredoxin reductase exists in two conformations, both of which are necessary for catalysis [Waksman, G., Krishna, T. S. R., Williams, C. H., Jr., & Kuriyan, J. (1994) *J. Mol. Biol.* 236, 800–816]. These factors make it likely that the mechanism of this enzyme is complex. The rapid reaction of enzyme with nicotinamide adenine dinucleotide phosphate, reduced form (NADPH) (the reductive half-reaction), proceeds in three phases. The first phase represents the formation of an NADPH–FAD charge transfer complex. The second phase involves FAD reduction, with loss of the NADPH–FAD charge transfer band. The third phase shows a slower decrease in absorbance at 456 nm and the formation of a reduced flavin–NADP<sup>+</sup> charge transfer band. These and other results indicate that NADP<sup>+</sup> and NADPH compete for the single binding site on oxidized and fully reduced enzyme and that NADP<sup>+</sup> release does not limit the third phase of reduction. Experiments that include examination of the reductive half-reactions of active-site mutants, having the active-site disulfide removed by mutating one or both of the active-site cysteines, indicate that the third phase does not represent reduction by a second equivalent of NADPH. Comparison of the rate constants and temperature dependence of the reductive half-reaction with those of turnover show that the reductive half-reaction is not solely rate-limiting in catalysis. The results suggest that wild type and each altered enzyme exists in a unique equilibrium of conformers. It is proposed that the third phase of the reductive half-reaction represents a flavin reduction event largely limited by the conformational change proposed in the structural work.

*Escherichia coli* thioredoxin reductase (EC 1.6.4.5) is a homodimer whose monomers have  $M_r = 35\,300$ . As a member of the pyridine nucleotide–disulfide oxidoreductase family, which also includes lipoamide dehydrogenase and glutathione reductase, thioredoxin reductase contains one FAD and one redox-active disulfide per monomer (Williams, 1992; Moore et al., 1964; Russel & Model, 1988; Zanetti & Williams, 1967). This enzyme catalyzes the reduction of a  $M_r = 11\,700$  protein, thioredoxin, by NADPH (Moore et al., 1964; Holmgren, 1968). During catalysis, electrons are passed from NADPH to flavin, from reduced flavin to the enzyme disulfide, and then from the newly formed enzyme dithiol to the disulfide on thioredoxin (Moore et al., 1964; Russel & Model, 1988; Zanetti & Williams, 1967). Steady-state kinetic studies have suggested that thioredoxin reductase proceeds via a ping-pong mechanism and that NADP<sup>+</sup> is an inhibitor competitive with NADPH (Williams, 1976; Prongay et al., 1989). However, other evidence indicates that thioredoxin reductase actually utilizes a ternary complex mechanism (Lennon & Williams, 1995, 1996). In contrast to lipoamide dehydrogenase and glutathione reductase that cycle in catalysis between the E<sub>ox</sub> and EH<sub>2</sub> states, enzyme monitored turnover shows that the spectrum of thioredoxin reductase during turnover is that of fully reduced flavin with

NADP(H) bound and thus the catalytic cycle is between four-electron-reduced and two-electron-reduced forms of the enzyme (Lennon & Williams, 1996). It should be noted the thioredoxin reductase from higher eukaryotes is like lipoamide dehydrogenase and glutathione reductase in structure and mechanism and is distinct from thioredoxin reductase from *E. coli* (Arscott et al., 1997).

The reduction of *E. coli* thioredoxin reductase by NADPH (termed the reductive half-reaction) has been studied by stopped-flow spectrophotometry. Massey et al. (1970) published results of a study of the reduction of thioredoxin reductase by one concentration of NADPH which showed that at 1.5 °C and pH 7.6 the enzyme is reduced in three steps. The first step was originally thought to be the transfer of one electron from NADPH to the flavin, although this step is interpreted in the present work as the formation of an NADPH–FAD charge transfer complex. This step was complete in the dead time of the stopped-flow instrument. The next two steps proceeded with observed rate constants of 44 s<sup>−1</sup> and 5.2 s<sup>−1</sup>, where the faster step represented flavin reduction. The slower step was thought to represent either the release of NADP<sup>+</sup> from an intermediate form of the enzyme or reduction of two-electron-reduced enzyme to four-electron-reduced (Massey et al., 1970).

The reductive half-reaction of thioredoxin reductase is potentially very complex for two reasons. First, thioredoxin reductase contains not only an FAD but also a redox-active disulfide (Zanetti & Williams, 1967). The midpoint potentials of the flavin and the active-site disulfide are separated by only 7 mV at pH 7.6 as calculated by proton slopes and

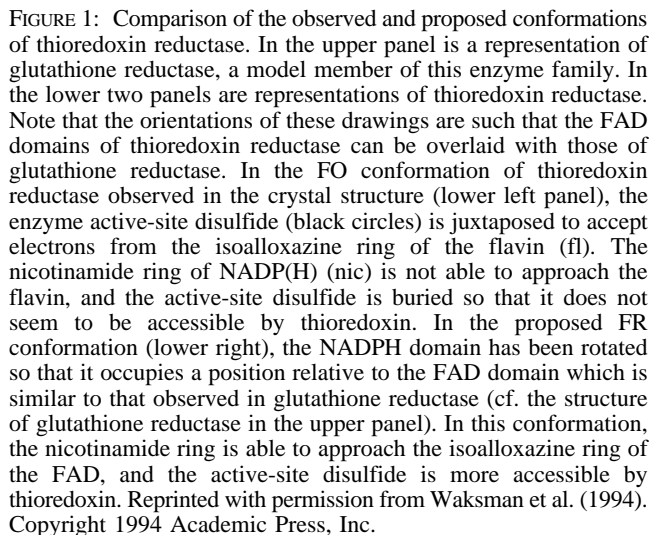
<sup>†</sup> This research was supported by the Department of Veterans Affairs (C.H.W.), by NIGMS Grant GM21444 (C.H.W.), and by the Pharmaceutical Sciences Training Program, University of Michigan (B.W.L.), which is funded by the National Institutes of Health.

\* To whom correspondence should be addressed: Medical Research Service, 151, VA Medical Center, 2215 Fuller Rd., Ann Arbor, MI 48105. (313) 769-7100, ext 5611; FAX (313) 761-7693.

<sup>®</sup> Abstract published in *Advance ACS Abstracts*, July 15, 1997.

$$\begin{array}{c}
 \text{NADPH} \\
 \begin{array}{c} \text{[ FAD} \\ \text{S} \\ \text{S} ]} \end{array} \xrightleftharpoons{k_{\text{on}}} \begin{array}{c} \text{NADPH} \\ \text{[ FAD} \\ \text{S} \\ \text{S} ]} \end{array} \xrightleftharpoons{k_{\text{FR}}} \begin{array}{c} \text{NADP}^+ \\ \text{[ FADH}_2 \\ \text{S} \\ \text{S} ]} \end{array} \xrightleftharpoons[k_{\text{ETB}}]{k_{\text{ETF}}} \begin{array}{c} \text{NADP}^+ \\ \text{[ FAD} \\ \text{SH} \\ \text{SH} ]} \end{array} \\
 \\
 \begin{array}{c} \text{NADP}^+ \updownarrow \\ k_{\text{PNO}} \end{array} \quad \begin{array}{c} \text{NADP}^+ \updownarrow \\ k_{\text{PNO}} \end{array} \\
 \\
 \begin{array}{c} \text{[ FADH}_2 \\ \text{S} \\ \text{S} ]} \xrightleftharpoons[k_{\text{ETB}}]{k_{\text{ETF}}} \begin{array}{c} \text{[ FAD} \\ \text{SH} \\ \text{SH} ]} \end{array} \\
 \\
 \begin{array}{c} k_{\text{on}}' \updownarrow \\ \text{NADPH} \end{array} \quad \begin{array}{c} k_{\text{on}}' \updownarrow \\ \text{NADPH} \end{array} \\
 \\
 \begin{array}{c} \text{[ NADPH} \\ \text{FADH}_2 \\ \text{S} \\ \text{S} ]} \xrightleftharpoons[k_{\text{ETB}}]{k_{\text{ETF}}} \begin{array}{c} \text{[ NADPH} \\ \text{FAD} \\ \text{SH} \\ \text{SH} ]} \end{array} \\
 \\
 k_{\text{FR}}' \updownarrow \\
 \begin{array}{c} \text{[ NADP}^+ \\ \text{FADH}_2 \\ \text{SH} \\ \text{SH} ]} \\
 \\
 \begin{array}{c} \text{NADP}^+ \updownarrow \\ k_{\text{PNO}}' \end{array} \\
 \\
 \begin{array}{c} \text{[ FADH}_2 \\ \text{SH} \\ \text{SH} ]} \end{array}
 \end{array}$$

The second reason the reductive half-reaction is potentially very complex involves structural features of this enzyme. For a more detailed explanation of these features, see Waksman et al. (1994). Briefly, in the crystal structures of the wild type and two mutant enzymes, it is not possible to bind pyridine nucleotide to the enzyme such that the nicotinamide ring is in a position to transfer a hydride to the isalloxazine ring of the flavin. Not only is it too far from the flavin but also the nicotinamide ring is not parallel to the flavin, and the active-site disulfide is blocking its access to the isalloxazine (Figure 1, lower left panel). Due to the buried position of the disulfide, there is also no obvious



way for the substrate thioredoxin to gain access to the enzyme active-site dithiol or to the flavin directly. We refer to this structure as the FO conformation because it is the conformation in which the reduced flavin can be oxidized by the enzyme disulfide. It was noted that while the dimerization of thioredoxin reductase was different from the other members of this enzyme family, the interface domain present in the other members being missing, thioredoxin reductase still shared a three-dimensional homology with the other family members. The graphics terminal was used to rotate the pyridine nucleotide domain of thioredoxin reductase 66° about the  $\beta$  sheet that connects it to the FAD domain (Waksman et al., 1994). This rotation causes the pyridine nucleotide and FAD domains to become juxtaposed as they are in glutathione reductase, a model member of the family (cf. upper and lower right panels of Figure 1). This accomplishes two things. One, the active-site disulfide of the enzyme moves out from the interior of the protein and

apparently becomes accessible to thioredoxin. By contrast, in the FO conformation actually observed in the crystal structure, the FAD and the redox-active disulfide are juxtaposed for efficient electron transfer. Two, the nicotinamide ring of NADP(H) bound to the enzyme moves closer to the flavin and becomes parallel to it, a position that is favorable for hydride transfer between NADPH and the flavin. Since this hypothetical conformation is favorable for flavin reduction by NADPH, we refer to it as the FR conformation. There are no major steric hindrances to the rotation modeled incrementally (Waksman et al., 1994). The properties of a stable mixed disulfide between thioredoxin reductase and thioredoxin indicate that it is held in the FR conformation (Wang et al., 1996). The complex has been crystallized and the structure is being studied (Lennon et al., 1997).

Given this potential for complexity, the reductive half-reaction was reexamined in the current work. Dependence of the observed rate constants of the three phases of reduction on the concentration of NADPH was studied, as was the effect of the presence of added NADP<sup>+</sup>. These results were compared with those from steady-state assays to try to identify the rate-limiting step(s) in catalysis. It was suggested earlier that the third phase of reduction may represent the reduction of two-electron-reduced enzyme by a second equivalent of NADPH, since reduction of wild-type thioredoxin reductase normally requires the addition of four electrons—two to reduce the FAD and two to reduce the active-site disulfide (Massey et al., 1970; Williams et al., 1991). To examine this idea, the reductive half-reaction was studied using partially reduced wild-type enzyme or using site-directed mutants of thioredoxin reductase in which the active-site disulfide, which consists of the residues Cys<sup>135</sup> and Cys<sup>138</sup>, was removed by mutating one or both of the cysteines. In both cases the enzyme would react with only 1 equiv of NADPH, in contrast to the oxidized wild-type enzyme. The results suggest that the third, slowest phase of the reductive half-reaction is not solely rate-limiting in catalysis, nor does it represent the release of NADP<sup>+</sup> or reduction of the enzyme by a second equivalent of NADPH. It is instead proposed that the third phase of reduction represents a flavin reduction event largely limited by the conformational change proposed in the structural work.

## MATERIALS AND METHODS

**Reagents.** NADP<sup>+</sup> (Sigma grade), NADPH (type III, enzymatically reduced), and protocatechuic acid (3,4-dihydroxybenzoic acid) were all purchased from Sigma. Protocatechuate dioxygenase was the generous gift of Dr. David P. Ballou of the Department of Biological Chemistry, University of Michigan. Sodium dithionite was purchased from Fluka Chemical Corp. All other reagents and buffers were of the highest quality available.

**Purification of *E. coli* Thioredoxin Reductase.** Bacteria containing wild-type enzyme and TrxR(Cys<sup>135</sup>,Ser<sup>138</sup>)<sup>1</sup> were grown in Mueller Hinton broth at 37 °C as previously described using a *trxB*<sup>−</sup> strain of *E. coli* (K1380) containing a high copy number plasmid which carried either the wild-type enzyme (pTRR1) or TrxR(Cys<sup>135</sup>,Ser<sup>138</sup>) mutant (pTRR43) gene (Mulrooney & Williams, 1994). Bacteria containing TrxR(Ser<sup>135</sup>,Cys<sup>138</sup>) were grown by previously published methods (Prongay et al., 1989). TrxR(Ala<sup>135</sup>,Ala<sup>138</sup>) and

TrxR(Ser<sup>135</sup>,Ser<sup>138</sup>) were grown in *E. coli* strain A326 transformed with pTRR120 and pTRR124, respectively, as previously described for other thioredoxin reductase mutants (Mulrooney & Williams, 1994). These two mutants contained an extraneous mutation, that of Glu<sup>70</sup> to Asp. In addition, one preparation of wild-type enzyme was grown in strain XL1-B[pTRR201], as previously described for thioredoxin reductase mutants (Mulrooney & Williams, 1994), and the enzyme from this preparation contained the same mutation. The wild-type (E70D) enzyme was used in the reductive half-reaction at 1 °C to obtain long-wavelength data and rapid-scan diode array spectra, and it should be noted that several reductive half-reaction experiments with true wild-type enzyme produced the same results at 456 nm as the experiment with the wild-type (E70D) enzyme. This finding and the fact that the conservative mutation of Glu<sup>70</sup> lies on the surface of the enzyme away from the active site support the conclusion that the extraneous mutation does not affect the enzyme's reductive half-reaction.

Wild type and all mutant enzymes were prepared as previously described (Lennon & Williams, 1995, 1996), except that the Pharmacia 2', 5'-ADP-Sepharose 4B column was eluted with a linear gradient of 0–1 M NaCl over 4 column volumes, with thioredoxin reductase eluting at about 0.75 M NaCl. Wild-type enzyme was quantitated using a value of  $\epsilon_{456} = 11\,300\text{ M}^{-1}\text{ cm}^{-1}$  (Williams et al., 1967). Mutant enzyme samples were quantitated by extinction coefficients determined by comparing the absorbance at the flavin peak at ~450 nm in the holoenzymes with the absorbance of the free flavin [ $\epsilon_{450} = 11\,300\text{ M}^{-1}\text{ cm}^{-1}$  (Beinert, 1960)] released by the addition of 0.2% SDS or 6 M guanidinium chloride (work by Donna M. Veine in this laboratory). The extinction coefficients determined are as follows: TrxR(Ser<sup>135</sup>,Cys<sup>138</sup>),  $\epsilon_{453} = 9160\text{ M}^{-1}\text{ cm}^{-1}$ ; TrxR-(Cys<sup>135</sup>,Ser<sup>138</sup>),  $\epsilon_{447} = 11\,700\text{ M}^{-1}\text{ cm}^{-1}$ ; TrxR(Ser<sup>135</sup>,Ser<sup>138</sup>),  $\epsilon_{450} = 11\,900\text{ M}^{-1}\text{ cm}^{-1}$ ; TrxR(Ala<sup>135</sup>,Ala<sup>138</sup>),  $\epsilon_{452} = 11\,300\text{ M}^{-1}\text{ cm}^{-1}$ .

**Anaerobiosis.** NADPH samples, quantified by absorbance ( $\epsilon_{340} = 6220\text{ M}^{-1}\text{ cm}^{-1}$ ) (Malcolm, 1980) were made anaerobic by bubbling for at least 20 min with ultrapure (99.999%) nitrogen which had been passed over an R & D Separations OT3-4 oxygen trap. To some samples 80  $\mu\text{M}$  protocatechuic acid and 0.04 unit/mL protocatechuate dioxygenase were added to remove trace oxygen. The results were unchanged whether protocatechuic acid and protocatechuate dioxygenase were present in the NADPH samples or not. Enzyme samples were made anaerobic in tonometers as previously described (Lennon & Williams, 1995). In experiments where NADP<sup>+</sup> was premixed with enzyme, the NADP<sup>+</sup> was placed in a side arm of the tonometer during

<sup>1</sup> Abbreviations: TrxR(Ser<sup>135</sup>,Cys<sup>138</sup>), site-directed mutant of thioredoxin reductase in which Cys<sup>135</sup> has been replaced with a serine; TrxR-(Cys<sup>135</sup>,Ser<sup>138</sup>), site-directed mutant of thioredoxin reductase in which Cys<sup>138</sup> has been replaced with a serine; TrxR(Ser<sup>135</sup>,Ser<sup>138</sup>), site-directed mutant of thioredoxin reductase in which both Cys<sup>135</sup> and Cys<sup>138</sup> have been replaced by serine; TrxR(Ala<sup>135</sup>,Ala<sup>138</sup>), site-directed mutant of thioredoxin reductase in which both Cys<sup>135</sup> and Cys<sup>138</sup> have been replaced by alanine; E<sub>ox</sub>, oxidized wild-type enzyme; E(FADH<sub>2</sub>)-(S)<sub>2</sub>, two-electron-reduced wild-type enzyme containing reduced flavin and a disulfide; E(FAD)-(SH)<sub>2</sub>, two-electron-reduced wild-type enzyme containing oxidized flavin and a dithiol; E<sub>red</sub>, four-electron-reduced wild-type enzyme.

anaerobiosis and was mixed with the enzyme once anaerobiosis was complete.

**Stopped-Flow Spectrophotometry.** The stopped-flow instrument and data collection and analysis methods used were described previously (Lennon & Williams, 1995). The reductive half-reaction with NADPH was studied by placing anaerobic oxidized thioredoxin reductase in one syringe and anaerobic NADPH samples in the other syringe. In cases where  $\text{NADP}^+$  was added prior to the experiment, it was included in both the enzyme and NADPH samples to prevent dilution of the  $\text{NADP}^+$  during mixing. The two solutions were mixed rapidly, and the reaction was monitored via the monochromator and the photodiode array. Experiments were done in 0.1 M sodium/potassium phosphate, pH 7.6, at either 1 or 25 °C. Buffer pH values for all experiments were adjusted at the same temperature at which they were used. Enzyme concentrations were 5–19  $\mu\text{M}$  after mixing, and concentrations of NADPH ranged from 10 to 520  $\mu\text{M}$  after mixing. Data were collected by a photodiode array (full spectra taken at 5.42 ms intervals), as well as by observing absorbance changes at single wavelengths using a monochromator and a photomultiplier. Due to the greater time resolution of the single-wavelength data, analysis of these data yield more accurate observed rate constants than are obtained from the photodiode array. Each reaction was repeated 3–5 times, and the fits resulting from each curve observed at the flavin peak were averaged for the final values of the observed rate constants. The fitted curves were extrapolated back for the 3–4 ms dead time of the stopped-flow instrument in order to more accurately determine the amplitudes of the phases, including the phase occurring in the dead time. Due to the small changes in absorbance and fast rates observed for the first phase of reduction, when necessary the rate constant for the first phase was fixed so that the extrapolated starting absorbance from the fit matched the observed starting absorbance of oxidized enzyme. Note that in these cases (where the observed rate constants are near  $1000 \text{ s}^{-1}$ ) the observed rate constants are at the limit of the experimental technique, and so greater uncertainty exists regarding these values than is indicated by the standard deviations. At the longer wavelengths (540 and 690 nm), due to the small absorbance changes and poor signal to noise ratio, the reaction traces were averaged together and corrected for a mixing artifact before fitting. Apparent  $K_d$  values were obtained from plots of observed rate constants versus concentration of NADPH assuming a rectangular hyperbolic function using the Marquardt–Levenberg algorithm in the curve-fitting function from SigmaPlot for Windows (Jandel Scientific, San Rafael, CA).

**Kinetic Simulation.** The differential equations describing the steps leading to the formation and decay of each species in a mechanism of interest were written. These equations were evaluated by a Runge–Kutta numerical method in Program A (developed by Chung-Yen Chiu, Rong Chang, Joel Dinverno, and David P. Ballou, University of Michigan). Using rate constants provided, the program calculates the concentration of enzyme species at various time points and displays an absorbance versus time trace based on the sum of the absorbances of all enzyme species as calculated from extinction coefficients provided. Detailed descriptions of the results of the kinetic simulations can be found in Appendices A and B in the supporting information.

**Steady-State Assays.** Assays contained 50 mM sodium/potassium phosphate, pH 7.6, 1.5 mM EDTA, and various concentrations of NADPH and thioredoxin. The reaction was started by the addition of 3.4 pmol of enzyme in a 10  $\mu\text{L}$  volume. Total assay volume was 1.0 mL. Assays were repeated 3–4 times at each set of substrate concentrations, and the results were averaged.

The course of the reaction was followed by monitoring the decrease in fluorescence of NADPH at 25 °C. A Perkin-Elmer MPF-44B fluorescence spectrophotometer with a temperature-controlled cuvette holder was used with an excitation wavelength of 340 nm and an emission wavelength of 456 nm. Reaction velocities were converted from percent relative fluorescence per unit time to concentration of NADPH per unit time by use of a standard curve, which was generated by reading the relative fluorescence of a series of freshly made NADPH stock solutions accurately quantitated by  $A_{340}$ . Nonlinear fits of velocity versus concentration of one substrate assuming a rectangular hyperbolic function were done by the Marquardt–Levenberg algorithm in the curve-fitting function from SigmaPlot for Windows (Jandel Scientific, San Rafael, CA) to obtain an apparent  $V_{\text{max}}$  at each concentration of the second substrate. These fitted results were plotted in double-reciprocal format when necessary to facilitate analysis. Secondary plots of  $V_{\text{max app}}$  versus concentration of the second substrate were analyzed in the same manner to obtain the  $V_{\text{max}}$  at saturating conditions for both substrates, as well as the  $K_m$  value for the second substrate. As had been done in previous steady-state kinetic analyses (Williams, 1976; Prongay et al., 1989), this analysis used the velocity equation for a ping-pong mechanism because the double-reciprocal plots displayed parallel lines, although recent work has indicated that a ping-pong mechanism is probably not correct for thioredoxin reductase (Lennon & Williams, 1995, 1996). As was mentioned in Lennon and Williams (1995), a ternary complex mechanism can display parallel lines in Lineweaver–Burk plots given certain assumptions (e.g., Palmer & Massey, 1968). This is because in those cases the steady-state velocity equation for a ternary complex mechanism simplifies to an equation that will yield parallel lines in a Lineweaver–Burk plot. We have assumed that this is the case for thioredoxin reductase. Thus, the values for  $V_{\text{max}}$  and  $K_m$  obtained are probably best described as apparent values.

**Temperature Dependence of the Reductive Half-Reaction.** Wild-type enzyme (5  $\mu\text{M}$ ) was rapidly mixed with 516  $\mu\text{M}$  NADPH (concentrations after mixing) at 1, 5, 10, 15, and 20 °C in 0.1 M sodium/potassium phosphate buffer that had been adjusted to pH 7.60 at 1 °C. Given that the phosphate buffering system in this range ( $\text{p}K_a = 7.20$ ) has a  $\Delta\text{p}K_a/^\circ\text{C}$  of  $-0.0028$  (Stoll & Blanchard, 1990), the calculated pH of the reaction at each temperature ranged from 7.59 at 5 °C to 7.53 at 20 °C. The concentration of NADPH is high enough that the observed rate constants should be maximal at all temperatures (see apparent  $K_d$  values in columns 2 and 9 of Table 2), and so the data should not reflect a temperature effect on the binding of NADPH. Data shown at 25 °C in Figure 6 were not obtained from this experiment but were instead taken from the reductive half-reaction at 25 °C mentioned above, at a concentration of 430  $\mu\text{M}$  NADPH and pH 7.6. These 25 °C data were not used in the linear regression shown in Figure 6 (described below) but were included on the plots to determine how closely they fall to

the theoretical line at 25 °C as extrapolated from the data between 1 and 20 °C.

Arrhenius plots were done by plotting  $\log(k/T)$  versus  $1/T$ , based on the equation  $\log(k/T) = \log(R/Nh) + \Delta S^\ddagger/2.303R - \Delta H^\ddagger/2.303RT$ , where  $k$  is the observed rate constant for the process of interest,  $T$  is the absolute temperature,  $R$  is the gas constant,  $N$  is Avogadro's number, and  $h$  is Planck's constant (Segel, 1975). The slope of this plot was used to obtain the value for  $\Delta H^\ddagger$ . The equation  $k = (RT/Nh) e^{(-\Delta G^\ddagger/RT)}$  was used to calculate  $\Delta G^\ddagger$  from the observed rate constant at each temperature, and then the equation  $\Delta G^\ddagger = \Delta H^\ddagger - T\Delta S^\ddagger$  was used to calculate  $\Delta S^\ddagger$  from the values of  $\Delta H^\ddagger$  and  $\Delta G^\ddagger$  (Segel, 1975). These values for  $\Delta S^\ddagger$  are in good agreement with those obtained from the y intercepts of the plots of  $\log(k/T)$  versus  $1/T$ .

**Partial Reduction of Thioredoxin Reductase.** For use in the rapid reaction study of the reductive half-reaction, wild-type thioredoxin reductase was partially reduced by 1.4 equiv of sodium dithionite as previously described (Lennon & Williams, 1995). As calculated using previously published methods (O'Donnell & Williams, 1983), enzyme at the start of the stopped-flow experiment contained 37% oxidized flavin, 26% reduced flavin, and a total of 37% one-electron and three-electron flavin semiquinone species (semiquinone species on enzyme containing a disulfide or a dithiol, respectively). Due to the small absorbance values and large amount of semiquinone formed, only the 456 nm data were useful. In calculating the  $\Delta\epsilon_{456}$  per phase in this experiment, the concentration of semiquinone was subtracted first, since semiquinone is not an active species in reactions of NADPH with thioredoxin reductase (Zanetti et al., 1968).

## RESULTS

**Reductive Half-Reaction of Wild-Type Thioredoxin Reductase.** Wild-type thioredoxin reductase was rapidly mixed in the stopped-flow spectrophotometer with various concentrations of NADPH at 1 °C, pH 7.6. The reaction proceeds in three phases as previously observed (Massey et al., 1970). Representative reaction traces are shown in Figure 2. The rate constants observed for the three phases were similar at all three wavelengths observed (456, 540, and 690 nm), although whether the absorbances increased or decreased differed, depending on what spectral species were forming or decaying. This will be discussed further below.

The first phase of reduction appears as a decrease at 456 nm accompanied by the formation of a broad band centered at about 550 nm but which also extends past 700 nm (Figure 3, spectrum 2). The formation of this species is nearly complete in the approximately 4 ms dead time of the stopped-flow instrument, and it contains about 17% of the total  $\Delta\epsilon_{456}$  (column 2 of Table 1). The spectral changes are consistent with the formation of an NADPH–FAD charge transfer complex (Blankenhorn, 1975). The observed rate constants obtained for this phase at 540 nm show a hyperbolic increase with increasing concentration of NADPH, with a maximal value of  $950 \pm 30 \text{ s}^{-1}$  and an apparent  $K_d$  of  $25 \pm 4 \text{ }\mu\text{M}$  (column 2 of Table 2). These values may have significant error caused by the large amount of the reaction that was complete in the dead time of the stopped-flow instrument, by the small changes in absorbance observed (Figure 2B), and by the fact that these rate constants are near the limit of the experimental technique. The saturability of these ob-

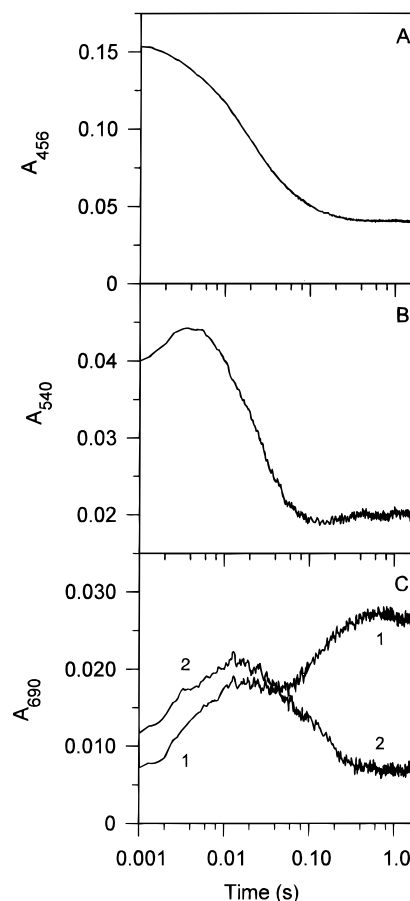
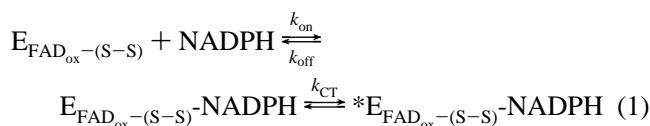


FIGURE 2: Changes in absorbance with increasing time in the reductive half-reaction of wild-type thioredoxin reductase at three wavelengths. Final concentration of enzyme is 17.1  $\mu\text{M}$ , pH 7.6, 1 °C. Panels A and B and curve 1 in panel C are from a reaction with a final concentration of 35.6  $\mu\text{M}$  NADPH. Curve 2 in panel C is from a reaction with a final concentration of 518  $\mu\text{M}$  NADPH.

served rate constants indicates that the formation of the NADPH–FAD charge transfer species is a separate, first-order event following binding (Strickland et al., 1975). Thus, eq 1 represents the most likely mechanism. The species \*E signifies the NADPH–FAD charge transfer species, and  $k_{CT}$  is the observed rate constant for the formation of that charge transfer species. Whether or not the charge transfer step is reversible is examined below. The initial NADPH–enzyme complex shown in eq 1 was not detected spectrally, both because it may be spectrally silent and because its formation is extremely fast. Thus, by the end of the dead time even if there were any spectral changes caused by the formation of this complex, they would be essentially complete and would be hidden within the spectral changes corresponding to the formation of the NADPH–FAD charge transfer band, which also forms very quickly.



The second phase of reduction involves the decay of the NADPH–FAD charge transfer complex as the flavin is reduced where the  $\Delta\epsilon_{456}$  comprises about 60% of the total change observed (column 2 of Table 1). The observed rate constant of the second phase shows a hyperbolic dependence on concentration of NADPH, with an apparent  $K_d$  of  $3.4 \pm$

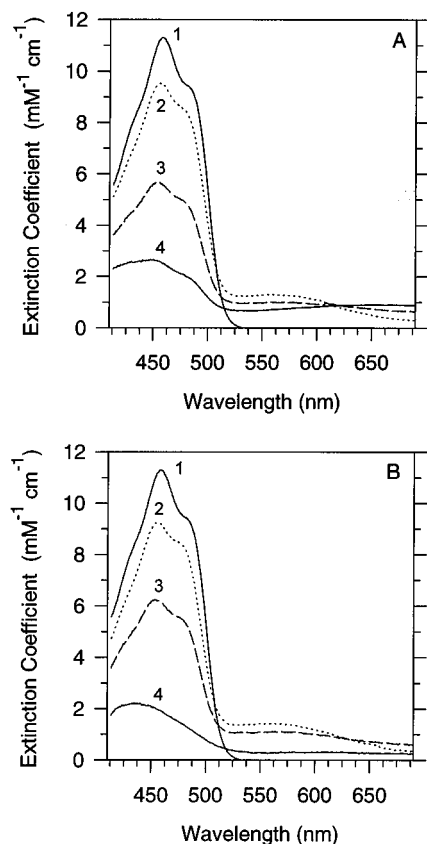
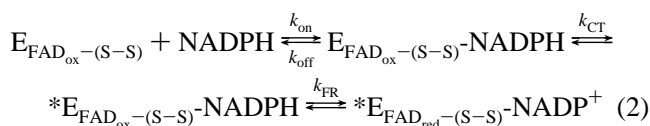


FIGURE 3: Spectra from the reductive half-reaction of wild-type thioredoxin reductase. Conditions are as for Figure 2. Panel A: 35.6  $\mu\text{M}$  NADPH. Spectra are (1) oxidized enzyme, (2) dead time (4.3 ms), (3) 2 half-lives of the second phase of reduction ( $k_{\text{FR}}$ ) and 0.4 half-life of the third phase of reduction ( $k_3$ ) (26.0 ms), and (4) final spectrum taken (2 min), all phases of reduction complete. Panel B: 518  $\mu\text{M}$  NADPH. Spectra are (1) oxidized enzyme, (2) dead time (4.3 ms), (3) 2 half-lives of the second phase of reduction ( $k_{\text{FR}}$ ) and 0.3 half-life of the third phase of reduction ( $k_3$ ) (20.6 ms), and (4) final spectrum taken (2 min), all phases of reduction complete.

0.5  $\mu\text{M}$  and a maximal observed rate constant of  $69 \pm 1 \text{ s}^{-1}$  (column 2 of Table 2). Spectrum 3 in Figure 3 shows the enzyme species observed after 2 half-lives of the second phase of reduction (75% complete) and after 0.3–0.4 half-life of the third phase of reduction (20–25% complete). Thus, these spectra largely represent the species present at the end of the second phase of reduction. This species has a lower level of the NADPH–FAD charge transfer band at 540 nm as compared to the dead-time spectrum (spectrum 2, Figure 3), indicating the loss of that band as flavin is reduced. Also, the extinction coefficient at 690 nm has increased, indicating some formation of a reduced flavin–NADP<sup>+</sup> charge transfer species (Zanetti & Williams, 1967; Blankenhorn, 1975; Massey & Palmer, 1962; Claiborne & Ahmed, 1989). The simplest mechanism which explains the results observed is that flavin reduction immediately follows formation of the NADPH–FAD charge transfer band. Equation 1 can be expanded, then, to include flavin reduction as shown in eq 2, where  $k_{\text{FR}}$  is the observed rate constant of the flavin



reduction step. This step should be reversible, since NADP<sup>+</sup>

can be reduced by reduced thioredoxin in the presence of thioredoxin reductase (Moore et al., 1964). Kinetic modeling of eq 2 has shown that when another step occurs (in this case charge transfer formation) between substrate binding and the observed step (flavin reduction), as long as the intermediate step is reversible, then the observed step will retain its hyperbolic dependence on the concentration of substrate (supporting information, Appendix A). Thus, the fact that  $k_{\text{FR}}$  is hyperbolically dependent on the concentration of NADPH suggests that the formation of the NADPH–FAD charge transfer complex is reversible. Note that while the simulations suggest that charge transfer formation is reversible, it is only known that the sum of the forward and backward rate constants for the charge transfer step is approximately  $950 \text{ s}^{-1}$ . The values of the individual forward and backward rate constants are not known. The simulations of this mechanism also show that the apparent  $K_d$  for the substrate as obtained from the plot of observed rate constant versus concentration of substrate for charge transfer formation and for flavin reduction tend to be higher and lower, respectively, than the true  $K_d$  (supporting information, Appendix A). Thus, it is likely that the  $K_d$  for NADPH binding to oxidized wild-type enzyme is between 25 and 3.4  $\mu\text{M}$ .

While the final species in eq 2 is a reduced flavin–NADP<sup>+</sup> charge transfer complex, spectrum 3 in Figure 3 does not fully reflect this, in that there is significant oxidized character. The long-wavelength absorbance in these spectra is also not purely that of a reduced flavin–NADP<sup>+</sup> charge transfer complex. There are two reasons for this. First, the spectra shown are not those of a pure species, since 25% of the second phase of reduction remains to be seen, and 20–25% of the third phase of reduction has already occurred. Second, the enzyme requires four electrons to be fully reduced. As written, eq 2 shows that the enzyme is only 50% reduced after the second phase of reduction. As mentioned earlier, partially reduced thioredoxin reductase is a mixture of four species at different redox states. No single two-electron-reduced species exists. Thus, the species shown in spectrum 3 is probably a combination of enzyme containing oxidized and reduced flavin and will have NADP<sup>+</sup> or NADPH bound to the extent dictated by the concentrations of NADP<sup>+</sup> and NADPH present and by their  $K_d$  values with the oxidized and reduced enzyme forms. Note that the displacement of NADP<sup>+</sup> by NADPH is facile (cf. spectrum 4 in Figure 3; see below).

The third phase of the reductive half-reaction is observed as a slower decrease in absorbance at 456 and 540 nm, as well as an increase at 690 nm at lower concentrations of NADPH ( $\leq 87 \mu\text{M}$ ) (curve 1, Figure 2C). This phase contains the remaining 23% of the observed  $\Delta\epsilon_{456}$  (column 2 of Table 1). The observed rate constant of this phase is independent of the concentration of NADPH (column 2 of Table 2), indicating that this phase is limited by a first-order process which is not affected by a preceding or succeeding binding step. The long-wavelength spectral characteristics of the species formed at the end of this phase are consistent with the significant formation of a reduced flavin–NADP<sup>+</sup> charge transfer complex at the lower concentrations of NADPH (Figure 3A, spectrum 4) (Zanetti & Williams, 1967; Blankenhorn, 1975; Massey & Palmer, 1962; Claiborne & Ahmed, 1989). The key observation is that during this phase the 690 nm absorbance increases when the NADPH con-

Table 1: Changes in Extinction Coefficients Observed during Each Phase of the Reductive Half-Reaction with Wild-Type, Partially Reduced Wild-Type, and Disulfide Mutant Thioredoxin Reductases<sup>a</sup>

	wild type	wild type + 180 $\mu$ M NADP <sup>+</sup>	wild type + 1.4 equiv of dithionite	TrxR- (Ser <sup>135</sup> ,Cys <sup>138</sup> )	TrxR- (Ser <sup>135</sup> ,Ser <sup>138</sup> )	TrxR- (Ala <sup>135</sup> ,Ala <sup>138</sup> )	TrxR- (Cys <sup>135</sup> ,Ser <sup>138</sup> )	wild type, 25 °C
[enzyme] ( $\mu$ M)	5.0 or 17.1 <sup>b</sup>	15.0	9.3 <sup>c</sup>	5.1 or 19.1 <sup>b</sup>	15.5	17.6	18.0	17.4
$\Delta\epsilon$ phase 1 ( $M^{-1} cm^{-1}$ )	-1550 $\pm$ 130	+430 to -850	-1400 $\pm$ 160	-1510 $\pm$ 140	-2050 $\pm$ 120	-2540 $\pm$ 230	-52 $\pm$ 86	-1250 <sup>d</sup>
% $\Delta\epsilon$ in phase 1	17	-5 to 9	25	21	21	27	1	14
$\Delta\epsilon$ phase 2 ( $M^{-1} cm^{-1}$ )	-5640 $\pm$ 120	-6810 $\pm$ 550	-2140 $\pm$ 120	-5610 $\pm$ 110	-7590 $\pm$ 130	-5350 $\pm$ 220	-1620 $\pm$ 230	-4400 $\pm$ 150
% $\Delta\epsilon$ in phase 2	60	87 to 75	39	78	77	56	19	49
$\Delta\epsilon$ phase 3 ( $M^{-1} cm^{-1}$ )	-2160 $\pm$ 210	-1470 $\pm$ 110	-2020 $\pm$ 90	-93 $\pm$ 46	-170 $\pm$ 50	-1610 $\pm$ 260	-6900 $\pm$ 200	-3400 $\pm$ 190
% $\Delta\epsilon$ in phase 3	23	19 to 16	36	1	2	17	81	38
$\epsilon_{final}$ ( $M^{-1} cm^{-1}$ )	1980 $\pm$ 130	2250 $\pm$ 30	3910 $\pm$ 110	2490 $\pm$ 110	1980 $\pm$ 170	1790 $\pm$ 50	2580 $\pm$ 210	2290 $\pm$ 70

<sup>a</sup> All reactions are with NADPH. The table refers to values as observed at the flavin peak. Values for  $\Delta\epsilon$  were obtained at saturating concentrations of NADPH ( $\sim$ 500  $\mu$ M). Temperature is 1 °C unless otherwise noted. Values are shown  $\pm$  1 $\sigma$ . <sup>b</sup> Experiments were done with two concentrations of enzyme. <sup>c</sup> Concentration of enzyme corrected for semiquinone. <sup>d</sup> There is no standard deviation because this value was artificially fixed to approximate the 1 °C value during analysis.

Table 2: Summary of the Rate Constants Observed in the Reductive Half-Reaction with Wild-Type, Partially Reduced Wild-Type, and Disulfide Mutant Thioredoxin Reductases<sup>a</sup>

	wild type	wild type + 180 $\mu$ M NADP <sup>+</sup>	wild type + 1.4 equiv of dithionite	TrxR- (Ser <sup>135</sup> ,Cys <sup>138</sup> )	TrxR- (Ser <sup>135</sup> ,Ser <sup>138</sup> )	TrxR- (Ala <sup>135</sup> ,Ala <sup>138</sup> )	TrxR- (Cys <sup>135</sup> ,Ser <sup>138</sup> )	wild type, 25 °C
[enzyme] ( $\mu$ M)	5.0 or 17.1 <sup>b</sup>	15.0	9.3	5.1 or 19.1 <sup>b</sup>	15.5	17.6	18.0	17.4
$k_{CT}$ ( $s^{-1}$ )	950 $\pm$ 30 <sup>d</sup>	520 $\pm$ 60 <sup>d</sup>	ND <sup>e</sup>	740 $\pm$ 190	400 $\pm$ 10	590 $\pm$ 40	425 <sup>d</sup>	ND <sup>f</sup>
$K_d$ app for $k_{CT}$ ( $\mu$ M)	25 $\pm$ 4	100 $\pm$ 30 <sup>d</sup>	ND	independent	21 $\pm$ 2	21 $\pm$ 12	independent	ND <sup>f</sup>
$k_{FR}$ ( $s^{-1}$ )	69 $\pm$ 1 <sup>h</sup>	57 $\pm$ 1	74 $\pm$ 5	29 $\pm$ 1	36 $\pm$ 1	68 $\pm$ 5	80 to 50	430 $\pm$ 20 <sup>i</sup>
$K_d$ app for $k_{FR}$ ( $\mu$ M)	3.4 $\pm$ 0.5	27 $\pm$ 3	9.7 $\pm$ 5.7	increasing, then decreasing	independent	independent	decreasing	81 $\pm$ 14
$k_3$ ( $s^{-1}$ )	9.0 $\pm$ 0.6	5.5 $\pm$ 1.1	9.4 $\pm$ 0.7	3.6 $\pm$ 1.6	3.7 $\pm$ 1.9	27 $\pm$ 3	10 to 7.5	53 $\pm$ 2
$K_d$ app for $k_3$ ( $\mu$ M)	independent	independent	independent	independent	independent	independent	decreasing	independent

<sup>a</sup> All reactions are with NADPH. The table refers to values as observed at the flavin peak except where noted.  $k_{CT}$  and  $k_{FR}$  refer to the first two phases of the reductive half-reaction (see text and eqs 1 and 2), and  $k_3$  refers to the third phase of the reductive half-reaction. Temperature is 1 °C unless otherwise noted. Values are shown  $\pm$  standard error except where noted. <sup>b</sup> Experiments were done with two concentrations of enzyme. <sup>c</sup> Concentration of enzyme corrected for semiquinone. <sup>d</sup> Data from 540 nm. <sup>e</sup> ND, not determined. <sup>f</sup> Not determined. This phase was essentially complete in the dead time. <sup>g</sup> Numerical values are apparent  $K_d$  values from a hyperbolic fit to the data. Otherwise, the entry describes the behavior of the observed rate constant for that phase with increasing concentration of NADPH. <sup>h</sup> Data from lower enzyme concentration experiment, which allowed use of a lower concentration of substrate. <sup>i</sup> The value determined from temperature dependence data is 590  $s^{-1}$  (Figure 6A). <sup>j</sup> Values are shown  $\pm$  1 $\sigma$ .

centration is low and decreases when the NADPH concentration is high (Figure 2C). This reflects the fact that a high concentration of NADPH can displace NADP<sup>+</sup> with loss of the reduced flavin–NADP<sup>+</sup> charge transfer complex (cf. spectrum 4 in panels A and B of Figure 3). At the higher concentration of NADPH, the final species does not represent either the NADPH–FAD or reduced flavin–NADP<sup>+</sup> charge transfer species observed previously. Instead, it is likely that the spectrum is that of fully reduced enzyme with NADPH bound. In the earlier study (Massey et al., 1970) it was reported that the dead-time species, i.e., the NADPH–FAD charge transfer complex, decayed at all wavelengths. Unlike what was observed in this work (Figure 2C, curve 1), no increasing absorbance was observed at the longer wavelengths by Massey et al. (1970) after the dead time. The reason for this is that only one high concentration of NADPH was used in that study (2.5 mM). At that concentration the NADPH would have efficiently competed with NADP<sup>+</sup> for the pyridine nucleotide binding site, thus precluding the formation of the reduced flavin–NADP<sup>+</sup> charge transfer complex. Instead, the absorbance during the second and third phases would have decreased at all wavelengths, as was reported.

Because a significant amount of the reduced flavin–NADP<sup>+</sup> charge transfer complex forms during the third phase of reduction at lower concentrations of NADPH (cf. spectra 3 and 4, Figure 3A), this phase probably does not represent the release of NADP<sup>+</sup>, contrary to what was postulated earlier

(Massey et al., 1970; Williams et al., 1991). As evidenced by the ability of NADPH to prevent formation of the reduced flavin–NADP<sup>+</sup> charge transfer band by displacing NADP<sup>+</sup>, NADP<sup>+</sup> release is quite facile.

*Reductive Half-Reaction of Wild-Type Thioredoxin Reductase in the Presence of Added NADP<sup>+</sup>.* Oxidized wild-type thioredoxin reductase was mixed with 180  $\mu$ M NADP<sup>+</sup> prior to use in the reductive half-reaction to explore how the reductive half-reaction is affected by NADP<sup>+</sup> and in order to confirm the conclusion that the third phase of reduction does not represent the release of NADP<sup>+</sup> from reduced enzyme. As was observed in the absence of NADP<sup>+</sup>, the first species formed upon mixing with NADPH is the NADPH–FAD charge transfer complex (Figure 4, spectrum 2). This phase is more difficult to detect at 456 nm and even less of the NADPH–FAD charge transfer complex formation is evident than in the absence of NADP<sup>+</sup>, since NADP<sup>+</sup> must first be displaced by NADPH and the flavin reduction that follows partially masks the changes due to charge transfer formation. At 540 nm, however, where the formation of this band can be more easily observed, an observed rate constant with a hyperbolic dependence on the concentration of NADPH is observed following a small lag phase. The maximal observed rate constant of 520  $\pm$  60  $s^{-1}$  is significantly smaller than that observed in the absence of NADP<sup>+</sup> and the apparent  $K_d$  has increased (Table 2). These results are probably due to competitive binding between NADP<sup>+</sup> and NADPH such that the formation of

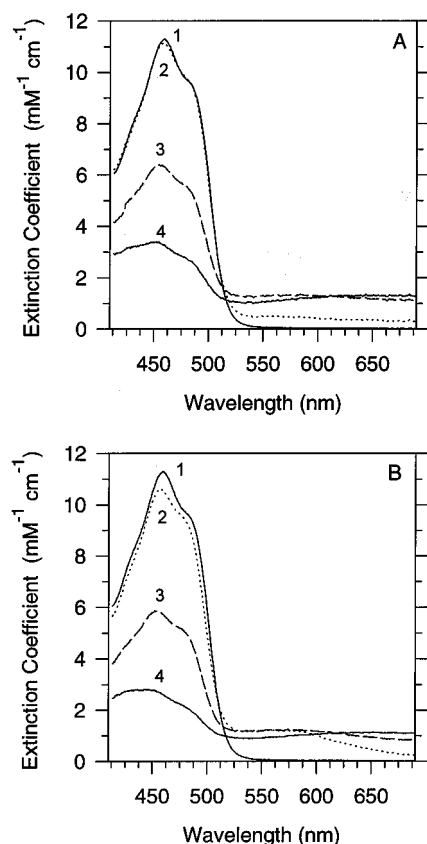


FIGURE 4: Spectra from the reductive half-reaction of wild-type thioredoxin reductase in the presence of added  $\text{NADP}^+$ . Conditions are  $15.0 \mu\text{M}$  enzyme and  $180 \mu\text{M}$   $\text{NADP}^+$  after mixing at pH 7.6,  $1^\circ\text{C}$ . Panel A:  $31.4 \mu\text{M}$  NADPH. Spectra are (1) oxidized enzyme, (2) dead time (4.3 ms), (3) 2 half-lives of the second phase of reduction ( $k_{\text{FR}}$ ) and 0.3 half-life of the third phase of reduction ( $k_3$ ) (46.3 ms), and (4) final spectrum taken (2 min), all phases of reduction complete. Panel B:  $231 \mu\text{M}$  NADPH. Spectra are (1) oxidized enzyme, (2) dead time (4.3 ms), (3) 2 half-lives of the second phase of reduction ( $k_{\text{FR}}$ ) and 0.3 half-life of the third phase of reduction ( $k_3$ ) (30.0 ms), and (4) final spectrum taken (2 min), all phases of reduction complete.

the charge transfer complex is no longer limited by how quickly the charge transfer species could form but also by how fast  $\text{NADP}^+$  was released so that NADPH could bind. The fact that the observed rate constant for this phase has decreased from  $950 \text{ s}^{-1}$  to  $520 \text{ s}^{-1}$  suggests that the rate constant of  $\text{NADP}^+$  release is at least  $520 \text{ s}^{-1}$ , since the NADPH–FAD charge transfer species cannot form faster than  $\text{NADP}^+$  vacates the pyridine nucleotide binding site. The increase in the apparent  $K_d$  for NADPH is expected in the presence of a competitively binding ligand. This agrees with steady-state results, which show that  $\text{NADP}^+$  is a competitive inhibitor of NADPH (Williams, 1976).

The second phase of reduction as observed at 456 and 540 nm still shows a decrease in absorbance with a hyperbolic dependence of the observed rate constant on the concentration of NADPH. The effect of added  $\text{NADP}^+$  on this phase is similar to that observed for the first phase of reduction in that the maximal value of the observed rate constant is decreased and the apparent  $K_d$  is increased (cf. columns 2 and 3 of Table 2). The spectral changes observed during this phase still reflect the reduction of flavin and some formation of a reduced flavin– $\text{NADP}^+$  charge transfer complex, but in the presence of additional  $\text{NADP}^+$ , the fraction of enzyme present as the reduced flavin– $\text{NADP}^+$

charge transfer complex following the second phase has increased (cf. spectrum 3 in panels A and B of Figures 3 and 4). This supports the conclusion made above that the enzyme species following the second phase of reduction actually consist of enzyme with either  $\text{NADP}^+$  or NADPH bound, and so in this case the higher concentration of  $\text{NADP}^+$  present simply causes the equilibrium to favor the formation of the reduced flavin– $\text{NADP}^+$  charge transfer complex.

During the third phase of reduction, the same general behavior is observed as in the absence of  $\text{NADP}^+$  at lower concentrations of NADPH in that the final species represents the further formation of a reduced flavin– $\text{NADP}^+$  charge transfer band (cf. spectra 3 and 4, Figure 4). However, higher levels of this species are now observed (cf. spectrum 4 in Figures 3 and 4). This supports the identification of the longer wavelength band present at the end of reduction by NADPH as being due to the reduced flavin– $\text{NADP}^+$  charge transfer band when the ratio of  $\text{NADP}^+$  to NADPH is high. Again, if the release of  $\text{NADP}^+$  was limiting the third phase of reduction, significant levels of the reduced flavin– $\text{NADP}^+$  charge transfer band would not form during this phase. The higher concentration of NADPH was less effective in displacing the  $\text{NADP}^+$  than in the absence of added  $\text{NADP}^+$  (cf. spectrum 4, Figures 3B and 4B). While the observed rate constant of the third phase of reduction at 456 nm is still independent of the concentration of NADPH, it has decreased to  $5.5 \pm 1.1 \text{ s}^{-1}$  (column 3 of Table 2).

**Reductive Half-Reaction of Partially Reduced Wild-Type Thioredoxin Reductase.** While the release of  $\text{NADP}^+$  has been ruled out as an explanation for the third phase of reduction, another possible explanation is that this phase represents the reduction of two-electron-reduced enzyme by a second equivalent of NADPH (Massey et al., 1970; Williams et al., 1991). In that case, partially reduced enzyme should show significantly smaller changes in absorbance during the third phase of reduction. To test this hypothesis, wild-type thioredoxin reductase was partially reduced by the addition of 1.4 equiv of dithionite prior to use in the reductive half-reaction. When this enzyme is rapidly mixed with various concentrations of NADPH, essentially the same kinetics are observed at 456 nm as with fully oxidized enzyme (Table 2, columns 2 and 4), but the amplitude of the second phase is significantly decreased (Table 1, columns 2 and 4). The fact that the third phase of reduction is a larger fraction of the total change in prereduced enzyme indicates that this phase is not simply the reduction of thioredoxin reductase by a second equivalent of NADPH. Since this enzyme sample contained significant levels of flavin semiquinone, the similarity of these kinetics to those obtained with fully oxidized enzyme confirm that the semiquinone form of this enzyme is not an active species in the reductive half-reaction (Zanetti et al., 1968).

**Reductive Half-Reaction of Disulfide Mutants.** Four disulfide mutants of thioredoxin reductase were also studied: TrxR(Ser<sup>135</sup>,Cys<sup>138</sup>), TrxR(Cys<sup>135</sup>,Ser<sup>138</sup>), TrxR(Ala<sup>135</sup>,Ala<sup>138</sup>), and TrxR(Ser<sup>135</sup>,Ser<sup>138</sup>). Each of these mutants, through the mutation of one or both of the active-site cysteines, lacks the redox-active disulfide. In this way one of the potentially complicating factors in interpreting the reductive half-reaction has been removed, namely, the presence of a second redox center. Since these mutants lack the redox-active disulfide, they cannot be reduced by more than 1 equiv of NADPH. It was hoped that this simplifica-



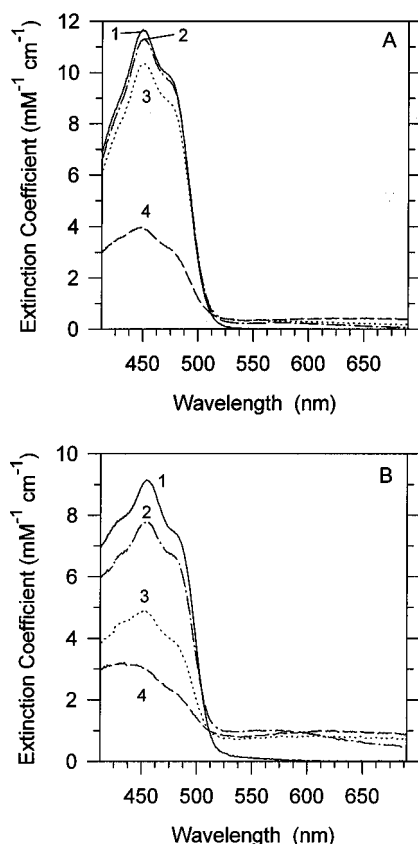


FIGURE 5: Spectra from the reductive half-reaction of disulfide mutants of thioredoxin reductase. Panel A: TrxR(Cys<sup>135</sup>,Ser<sup>138</sup>). Conditions are 18.0  $\mu$ M enzyme and 73.1  $\mu$ M NADPH after mixing at pH 7.6, 1 °C. Spectra are (1) oxidized enzyme, (2) dead time (4.3 ms), (3) 2.3 half-lives of the second phase of reduction ( $k_{FR}$ ) and 0.5 half-life of the third phase of reduction ( $k_3$ ) (20.6 ms), and (4) final spectrum taken (2 min), all phases of reduction complete. Panel B: TrxR(Ser<sup>135</sup>,Cys<sup>138</sup>). Conditions are 19.1  $\mu$ M enzyme and 39.1  $\mu$ M NADPH after mixing at pH 7.6, 1 °C. Spectra are (1) oxidized enzyme, (2) dead time (4.3 ms), (3) 1.9 half-lives of the second phase of reduction ( $k_{FR}$ ) and 0.2 half-life of the third phase of reduction ( $k_3$ ) (42.2 ms), and (4) final spectrum taken (2 min), all phases of reduction complete.

tion would help confirm that the third phase of reduction in wild-type thioredoxin reductase is not related to the reduction of the enzyme by a second equivalent of NADPH. As was observed with wild-type enzyme, the reductive half-reactions of all four mutants with NADPH at 1 °C contain three phases of decreasing absorbance at the flavin peak (Tables 1 and 2). This supports the conclusion that the third phase of reduction does not involve the reduction of the flavin by a second equivalent of NADPH. As was observed for wild-type enzyme, the reduced mutant enzymes appear to rapidly exchange NADPH for NADP<sup>+</sup>. As the concentration of NADPH increases, the final enzyme species observed lose long-wavelength character, presumably as NADP<sup>+</sup> is displaced from the reduced enzyme by NADPH, thus preventing the formation of the reduced flavin–NADP<sup>+</sup> charge transfer band.

While the reductive half-reactions of all four mutant enzymes did contain three phases of reduction, and the presence of the NADPH–FAD and reduced flavin–NADP<sup>+</sup> charge transfer bands were observed (e.g., Figure 5; cf. Figure 3), there were differences from wild-type enzyme (cf. column 2 with columns 5–8 in Tables 1 and 2). The observed rate constants, as well as their concentration dependencies, differed between the mutants and wild-type

enzyme, as well as among the mutants themselves. Note that none of the mutants displayed second-order kinetics for  $k_{CT}$ . This supports the conclusion that the formation of the NADPH–FAD charge transfer complex is a separate event following binding. However, as was done with wild-type enzyme, the rate constants for this first phase of reduction were fixed during analysis such that the starting absorbance returned by the computer fit matched the observed starting absorbance for the oxidized enzymes. While this procedure yielded more reasonable rate constants for the first phase than those fits in which the observed rate constant was allowed to vary freely, it may also introduce some error in the data (see Enthalpy of Activation in the Reductive Half-Reaction of Wild-Type Thioredoxin Reductase below). Conclusions regarding the first phase of reduction should be viewed with this in mind.

The most striking changes observed in the reductive half-reactions using the mutant enzymes are observed in TrxR-(Cys<sup>135</sup>,Ser<sup>138</sup>). In the other three mutant enzymes, the changes in extinction observed during each of the three phases of reduction were approximately the same magnitude as observed in wild-type enzyme except that phase 3 represented a smaller proportion of the change in extinction (columns 5–7, Table 1). In TrxR(Cys<sup>135</sup>,Ser<sup>138</sup>), on the other hand, while the species following the first phase of reduction still exhibits the same NADPH–FAD charge transfer characteristics observed in wild-type enzyme and in the other mutant enzymes, the  $\Delta\epsilon$  observed at the flavin peak during this phase is significantly decreased (Table 1, column 8, and Figure 5A, spectrum 2). It is also clear that the long-wavelength extinction coefficients of all charge transfer species have decreased significantly (Figure 5A), in contrast to the observation with the other mutants (Figure 5B and Table 1, columns 5–7) and in wild-type enzyme (cf. Figure 3). The second phase of reduction has also decreased significantly in amplitude in this mutant (Table 1, column 8, and Figure 5A, spectrum 3) and indeed is not distinguishable from the first phase of reduction at low concentrations of NADPH. The third phase of reduction at all concentrations of NADPH contains the majority of the change in extinction (Table 1, column 8), and spectrum 4 in Figure 5A shows that significant flavin reduction has occurred, with the concomitant formation of a reduced flavin–NADP<sup>+</sup> charge transfer complex at lower concentrations of NADPH. It will be discussed below how these observations lead to the idea that the third phase of reduction is largely limited by the proposed conformational change.

*Comparison of Wild-Type Thioredoxin Reductase Rapid Reaction Data to Steady-State Data.* In order to determine if any step of the reductive half-reaction is rate-limiting in turnover, it is necessary to compare the observed rate constants for the reductive half-reaction with steady-state kinetic parameters under similar conditions. The steady-state kinetic parameters for wild-type thioredoxin reductase have been determined previously (second and third columns of Table 3) (Williams, 1976; Prongay et al., 1989). There was a significant difference in the  $V_{max}$  values between these experiments, so the values were redetermined in this work (third column, Table 3). The value for  $V_{max}$  obtained was in good agreement with the result from Williams (1976), and so a value of  $k_{cat} = 33 \text{ s}^{-1}$  is used for thioredoxin reductase under these conditions.

Table 3: Steady-State Kinetic Parameters of Wild-Type Thioredoxin Reductase<sup>a</sup>

steady-state kinetic parameter	Williams (1976)	Prongay et al. (1989)	this work (± std error)
turnover number [nmol min <sup>-1</sup> nmol of TrxR <sup>-1</sup> ]	2000	1320	2010 ± 140
<i>K<sub>m</sub></i> NADPH (μM)	1.2	1.25	2.69 ± 0.59
<i>K<sub>m</sub></i> thioredoxin (μM)	2.8	2.89	3.68 ± 0.63

<sup>a</sup> Values from the present work are obtained by nonlinear fitting methods assuming a ping-pong mechanism and so are best described as apparent values (see Materials and Methods). Units for the turnover number are nanomoles of thioredoxin reduced per minute per nanomole of thioredoxin reductase.

The reductive half-reaction with NADPH was performed at 25 °C so that the rate constants obtained could be compared to the steady-state turnover number (column 9, Tables 1 and 2). The initial formation of the charge transfer species, as well as a large portion of the second phase of reduction, was fast enough to be complete in the dead time. This made it necessary to fix the rate constant of the second phase when fitting the reaction trace such that the extrapolated starting absorbance for the second phase matched what was expected on the basis of the 1 °C results. The observed rate constant obtained in this manner for the second phase of reduction showed saturability, with a maximum value of  $430 \pm 20 \text{ s}^{-1}$  and an apparent  $K_d$  of  $81 \pm 14 \text{ μM}$ . This is much too fast to be rate-limiting in catalysis (cf. Table 3). Given the potential for error in the analysis used, the larger apparent  $K_d$  for this phase as compared to 1 °C may partly be a result of the method used to fit the data. The observed rate constant of the third phase of reduction was essentially independent of the concentration of NADPH, with a value of  $53 \pm 2 \text{ s}^{-1}$ . Thus, the third phase of reduction represents the slowest competent step in the reductive half-reaction, but since it also is faster than  $k_{\text{cat}} = 33 \text{ s}^{-1}$ , it is clear that this step is not solely rate-limiting in turnover.

**Enthalpy of Activation in the Reductive Half-Reaction of Wild-Type Thioredoxin Reductase.** Since it was difficult to analyze the data at 25 °C due to the fast reaction rates, information from a study of the temperature dependence of the reductive half-reaction was used to check the accuracy of the values for the observed rate constants of the second and third phases of reduction at 25 °C just described. Arrhenius plots of the observed rate constants for these two phases are linear from 5 to 20 °C, indicating that there is no temperature-induced conformational change which affects the observed rate constant (Figure 6). The two 25 °C values (depending on how those reaction traces were fit) for the observed rate constant of the second phase of reduction obtained in the experiment described in the previous section fall on opposite sides of the theoretical line, indicating that the 25 °C values did contain some error introduced by the analysis method (Figure 6A). The plot predicts an observed rate constant at 25 °C of  $590 \text{ s}^{-1}$  for the second phase of reduction. The observed value for the third phase of reduction, on the other hand, was clearly not affected by the fitting method (Figure 6B).

The thermodynamic values obtained from these plots are shown in Table 4. Such data can indicate whether the transition state limiting a step in the reductive half-reaction is the same as the transition state that limits turnover. The differences between the pre-steady-state and steady-state

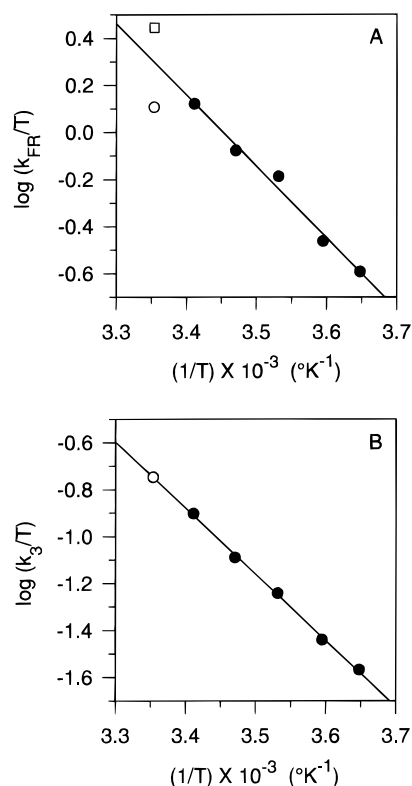


FIGURE 6: Temperature dependence of the reductive half-reaction of wild-type thioredoxin reductase. Conditions are 5 μM enzyme and 516 μM NADPH, pH 7.6. Lines are linear regressions of the filled circles only. Panel A: Temperature dependence of  $k_{FR}$ . Filled circles are data from the temperature dependence experiment. The open circle is the rate constant observed at 25 °C in the reductive half-reaction experiment using 430 μM NADPH in which the rate constant for this phase was fixed during analysis (see text). The open square is the same experiment in which the rate constant was not fixed during analysis. Panel B: Temperature dependence of the observed rate constant of the third phase of reduction. Filled circles are data from the temperature dependence experiment. The open circle is the rate constant observed at 25 °C in the reductive half-reaction experiment mentioned above in which the value of  $k_{FR}$  was fixed during analysis.

Table 4: Thermodynamic Parameters of Two Phases of the Reductive Half-Reaction and of Turnover with Wild-Type Thioredoxin Reductase<sup>a</sup>

kinetic parameter observed	$\Delta H^\ddagger$ (cal/mol)	$\Delta G^\ddagger$ (cal/mol)	$\Delta S^\ddagger$ [(cal/mol K)]
$k_{FR}$	$13\,900 \pm 930$	$13\,700 \pm 40$	$0.71 \pm 0.15$
$k_3$	$12\,900 \pm 300$	$15\,000 \pm 70$	$-7.40 \pm 0.05$
turnover number	10 000	$15\,200 \pm 270$	-18.2

<sup>a</sup> Values are from the analysis shown in Figure 6. Original turnover data are from Williams (1976). Where applicable, values are shown ± standard error.

activation enthalpies are small but probably real, and the activation entropies are clearly different. Thus, the transition state limiting in turnover is not identical to the transition state in either the second or third phase of the reductive half-reaction.

## DISCUSSION

**Proposed Role of the Putative Conformational Change in the Reductive Half-Reaction of Thioredoxin Reductase.** This study of the reductive half-reaction was an attempt to understand the mechanism of a well-studied enzyme at a

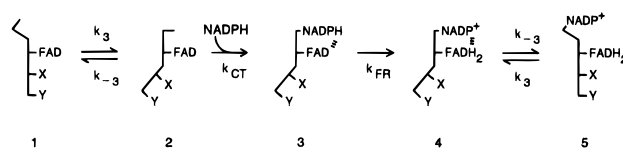
more detailed level. Two important characteristics of the mechanism have already been investigated. First, the enzyme utilizes a ternary complex (Lennon & Williams, 1995). Second, the catalytic cycle is between four-electron-reduced and two-electron-reduced forms of the enzyme (Lennon & Williams, 1996). These findings led to the proposal of a working hypothesis mechanism (Williams, 1995; Lennon & Williams, 1996). The mechanism reflects the postulate that only those molecules in the FR conformation can react immediately with NADPH, and thus, molecules in the FO conformation must undergo the conformational change to allow NADPH and FAD to interact (cf. Figure 1). A catalytic cycle begins with the enzyme in the FO conformation and in the E(FAD)–(SH)<sub>2</sub> state. NADPH binds and rotation to the FR conformation must occur before flavin can be reduced. With the enzyme in the FR conformation, dithiol–disulfide interchange can take place with the substrate, thioredoxin. Finally, the enzyme must return to the FO conformation to allow the electrons to be passed from the reduced flavin to the disulfide yielding E(FAD)–(SH)<sub>2</sub> (Williams, 1995; Lennon & Williams, 1996).

The proposal that two conformations are necessary for catalysis (Waksman et al., 1994) means that the reductive half-reaction would necessarily involve at least one rotation and one counterrotation to allow NADPH and the redox-active disulfide to alternately access the flavin (Figure 1). Our experiments using wild-type enzyme show that NADP<sup>+</sup> dissociation does not limit the third phase of the reductive half-reaction. The study of the reductive half-reaction of partially reduced enzyme and of mutants of the active-site disulfide in this work have also eliminated reduction of the enzyme by a second equivalent of NADPH as giving rise to the third phase of the reaction. Interjecting a historical note, these studies were essentially complete before the structure was known. Given the structural features of which we are now aware, the proposed conformational change is the prime candidate for the process ascribable to the slow step.

This view is supported by simulations of Scheme 1 (supporting information, Appendix B). As outlined above, since the original proposal of Scheme 1 (Williams et al., 1991) we have come to realize that the reduced flavin–disulfide electron equilibration step must include the proposed conformational change in order to bring the disulfide near the flavin for electron transfer. Thus, the simple electron transfer step  $k_{\text{ETF}}$  in Scheme 1 must consist of at least two separate steps: rotation and electron transfer. Similarly,  $k_{\text{ETB}}$  must consist of electron transfer followed by rotation back to the FR conformation. Simulations of Scheme 1 have suggested that all the step(s) involving the equilibration of electrons between the flavin and the disulfide are probably slower than  $k_{\text{FR}}$  (supporting information, Appendix B). It is not difficult to believe that the actual electron transfer step is indeed fast, as it is in other members of this enzyme family (Benen et al., 1992; Rietveld et al., 1994). Thus, it is probably the conformational change that is slower than  $k_{\text{FR}}$ , and so it is possible that the proposed conformational change is limiting at some point in the reductive half-reaction.

This idea is further supported by the reductive half-reactions of the mutant thioredoxin reductases. An explanation for the presence of three phases of reduction in the mutant enzymes is suggested by the different levels of charge transfer species formed among the mutant enzymes and by the properties of the two conformations proposed for

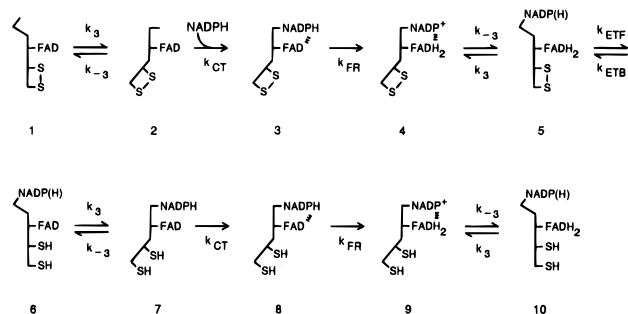
Scheme 2: Mechanism for the Reductive Half-Reaction of Mutant Thioredoxin Reductases<sup>a</sup>



<sup>a</sup> Since this mechanism applies to all the disulfide mutants, -X and -Y can represent -OH, -SH, or -CH<sub>3</sub>, depending on which mutant is being considered. The schematic enzyme backbone is bent to indicate which proposed conformation is present. When the pyridine nucleotide binding site is angled away from the flavin and the active-site residues (-X and -Y) are near the flavin, the enzyme is in the FO conformation (species 1 and 5). When the active-site residues are angled away from the flavin and the pyridine nucleotide binding site is near the flavin, the enzyme is in the proposed FR conformation (species 2–4). Charge transfer interactions are indicated by hatch marks between the flavin and pyridine nucleotide. The rate constants are identified as follows:  $k_3$ , rate constant for the third phase of reduction, here depicted as the rate constant for the conversion of the FO to the FR conformation;  $k_{-3}$ , rate constant for the conversion of the FR to the FO conformation;  $k_{\text{CT}}$ , rate constant for NADPH–FAD charge transfer formation (first phase of the reductive half-reaction);  $k_{\text{FR}}$ , rate constant for flavin reduction (second phase of the reductive half-reaction).

thioredoxin reductase. The FO conformation actually observed in the crystal structure does not allow the nicotinamide ring of NADP<sup>+</sup> (and presumably NADPH) to be juxtaposed for charge transfer formation with the isoalloxazine ring of the flavin; it is only the proposed FR conformation that is able to form a charge transfer complex involving flavin and pyridine nucleotide (Waksman et al., 1994). Thus, in TrxR-(Cys<sup>135</sup>,Ser<sup>138</sup>), where very low levels of flavin–pyridine nucleotide charge transfer interactions are observed and where the first phase of reduction is almost nonexistent, it appears that very little of the enzyme is present in the FR conformation. Conversely, in the other mutant enzymes, where significant flavin–pyridine nucleotide charge transfer interactions are observed and where the first phase of reduction is more visible, it is suggested that most of the enzyme is present in the FR conformation. We propose that in solution the two conformations postulated for thioredoxin reductase are in a dynamic equilibrium, and so the enzyme molecules that are not present in the FR conformation will exist in the FO conformation. Thus, there will be a balance between the two conformations, which apparently differs among the mutant enzymes. The fact that the crystal structure shows only the FO conformation is a consequence of that structure being favored as molecules are packed into the crystal (Waksman et al., 1994).

The ideas outlined above have been used to create a working hypothesis mechanism for the reductive half-reaction of the mutant thioredoxin reductases (Scheme 2). In this mechanism, oxidized enzyme is present initially in both the FO and FR conformations (species 1 and 2). NADPH is able to bind and rapidly form the NADPH–FAD charge transfer complex with the enzyme in the FR conformation, giving rise to the first phase of the reductive half-reaction. The enzyme that has formed the NADPH–FAD charge transfer complex (species 3) is now able to undergo flavin reduction, giving rise to the second phase of the reductive half-reaction. Meanwhile, the fraction of the oxidized enzyme that was originally in the FO conformation (species 1) is able to rotate to the FR conformation with some relatively slow rate constant ( $k_3$ ). Once it has assumed the

Scheme 3: Mechanism for the Reductive Half-Reaction of Wild-Type Thioredoxin Reductase<sup>a</sup>

<sup>a</sup> As in Scheme 2, the schematic enzyme backbone is bent to indicate whether the FO or FR conformation is present. Charge transfer interactions are indicated by hatch marks between the flavin and pyridine nucleotide. The rate constants are identified as follows:  $k_3$ , rate constant for the third phase of reduction, here depicted as the rate constant for the conversion of the FO to the FR conformation;  $k_{-3}$ , rate constant for the conversion of the FR to the FO conformation;  $k_{CT}$ , rate constant for NADPH–FAD charge transfer formation;  $k_{FR}$ , rate constant for flavin reduction;  $k_{ETB}$ , rate constant for electron transfer between the two enzyme redox centers in the forward direction;  $k_{ETF}$ , rate constant for electron transfer between the two enzyme redox centers in the backward direction. It is not known if any of these rates differ between oxidized and partially reduced enzymes. The pyridine nucleotide bound to species 5 and 6 is not shown specifically as NADP<sup>+</sup> or NADPH because it is not known at which point NADP<sup>+</sup> is released and the second equivalent of NADPH binds. This uncertainty makes no difference in the spectra of the species in question, since no charge transfer interactions should exist in those species. Species 10 is also not shown with a specific form of pyridine nucleotide bound, since it is shown that NADP<sup>+</sup> and NADPH freely exchange on the reduced enzyme.

FR conformation (species 2), NADPH–FAD charge transfer formation and flavin reduction occur. Since both of these steps are faster than the rate ascribed to the conformational change, the conformational change would be the rate-limiting step in the reduction of the enzyme present in the FO conformation, thus giving rise to the third phase of the reductive half-reaction. When reduction is complete, the enzyme will all be present in the FR conformation (species 4). However, the equilibrium between the FO and FR conformations will still exist, probably with a  $K_{eq}$  value similar to that observed with oxidized enzyme. This is supported by the fact that fully reduced TrxR(Cys<sup>135</sup>,Ser<sup>138</sup>) still has very low long-wavelength extinction. The flavin spectrum of enzyme in the FO conformation (species 5) should not be greatly affected by whether NADPH or NADP<sup>+</sup> is bound to it, since in that conformation the pyridine nucleotide would not be near the flavin (Waksman et al., 1994).

Scheme 3 represents a mechanism for the reductive half-reaction of wild-type thioredoxin reductase that is simply an expansion of the ideas depicted in Scheme 2 to allow for the presence of the active-site disulfide in wild-type enzyme. The general idea that the second and third phases of the reductive half-reaction of thioredoxin reductase are caused by flavin reduction in enzyme molecules in the FR and FO conformations, respectively, can also be used to explain the presence of three phases in the reductive half-reaction using partially reduced wild-type enzyme. Since partially reduced wild-type enzyme exists as an equilibrium of four redox states [ $E_{ox}$ ,  $E(FADH_2)-(S)_2$ ,  $E(FAD)-(SH)_2$ , and  $E_{red}$ ] (O'Donnell & Williams, 1983), enzyme species containing oxidized flavin [ $E_{ox}$  and  $E(FAD)-(SH)_2$ ] would be present.

Table 5: Apparent Equilibrium Constants for the FR and FO Conformations of Thioredoxin Reductase<sup>a</sup>

enzyme	$K_{eq}$ (FR/FO) ( $\Delta\epsilon$ phase 2/ $\Delta\epsilon$ phase 3)	$\Delta G^\circ$ , pH 7.6 (kcal/mol)
TrxR(Ser <sup>135</sup> ,Cys <sup>138</sup> )	60	−2.2
TrxR(Ser <sup>135</sup> ,Ser <sup>138</sup> )	45	−2.1
TrxR(Ala <sup>135</sup> ,Ala <sup>138</sup> )	3.3	−0.65
wild type	2.6	−0.52
TrxR(Cys <sup>135</sup> ,Ser <sup>138</sup> )	0.23	0.80

<sup>a</sup> The table was generated under the assumptions shown in Schemes 2 and 3 and described in the text. Values for the changes in extinction coefficient for the second and third phases of reduction are from Table 1. Values in the third column are calculated from the equation  $\Delta G^\circ = -RT \ln (K_{eq})$ .

These species would exhibit three phases of reduction (Scheme 3).

Note that for both wild type and all mutant enzymes the observed rate constant  $k_3$  was either independent of the concentration of NADPH or it decreased (Table 2). This is in agreement with the mechanisms in Schemes 2 and 3, because a conformational change followed by a binding event can exhibit a decreasing observed rate constant with increasing concentration of the ligand (Schopfer et al., 1988). Since this decrease can be very small (Fersht, 1985), it may be indistinguishable from concentration independence. Note that it is probably simplistic to assume that this third phase of the reductive half-reaction is influenced solely by the proposed conformational change. Given the complexity of the mechanisms proposed (Schemes 2 and 3), it is likely that the third phase of reduction actually represents a mixture of rate constants which is somewhat different among the enzymes studied.

The mechanism proposed states that those enzymes which exist largely in the FR conformation will have the most significant extinction changes in the first two phases of reduction, while those enzymes which exist largely in the FO conformation will have the most significant extinction changes in the third phase of reduction. If the amplitude of the first phase of reduction is discounted as being due to a charge transfer process and not actual flavin reduction, then the fraction of the extinction change at the flavin peak in the second phase of reduction may indicate how much enzyme is in the FR conformation, and the fraction of  $\Delta\epsilon$  in the third phase of reduction may indicate how much enzyme is in the FO conformation. This can give a measure of the equilibrium constant between the FR and FO enzyme forms (Table 5) and so provides a more quantitative value to the empirical observation that TrxR(Ser<sup>135</sup>,Cys<sup>138</sup>) (Figure 5B) and wild-type enzyme (Figure 3) are stabilizing more of the FR conformation, while TrxR(Cys<sup>135</sup>,Ser<sup>138</sup>) is stabilizing more of the FO conformation (Figure 5A). Using these approximate  $K_{eq}$  values, it can be seen that the  $\Delta G^\circ$  at pH 7.6 changes by  $\leq 3$  kcal/mol over the range of enzymes studied. Thus, there is not a large difference in energy between the extremes of the FR/FO equilibrium values shown in Table 5.

**Effect of Mutation on the Reductive Half-Reaction.** The reductive half-reactions of the active-site mutants were studied in order to determine if the removal of the active-site disulfide abolished the third phase of reduction, as would be predicted if the third phase of reduction in wild-type enzyme involved reduction by a second equivalent of

NADPH. However, further complications have been introduced by the mutations, which result in changes in the polarity of the active site and replace Cys with the less readily ionized Ser. Both polarity and charge can have important effects on chemical and structural aspects of enzymes. In any case, it is certain that the mutation of the active-site disulfide in thioredoxin reductase has an effect on the mechanism by which the enzyme is reduced (Tables 1 and 2).

It was observed in earlier studies using other techniques (Prongay et al., 1989; Prongay & Williams, 1990, 1992) that mutation of Cys<sup>138</sup> to Ser causes the largest changes in the flavin properties. In those studies, the changes were thought to be due to the modulation of the flavin environment by residue 138, which is known to be close to the flavin in the crystal structure. It is now proposed, however, that the reduction of flavin can only occur in the postulated FR conformation, in which residues 135 and 138 are no longer near the flavin. Thus, the effects on the reductive half-reaction caused by mutation of the active-site residues are probably not a result of the direct modulation of the flavin environment by the residue at position 138. For example, TrxR(Ser<sup>135</sup>,Ser<sup>138</sup>) behaves more like TrxR(Ser<sup>135</sup>,Cys<sup>138</sup>) than like TrxR(Cys<sup>135</sup>,Ser<sup>138</sup>) (Tables 1 and 2, columns 5, 6, and 8). If the effect of mutation was solely based on direct perturbation of the flavin environment by the mutated residues, the properties of the double serine mutant should have more closely resembled those of TrxR(Cys<sup>135</sup>,Ser<sup>138</sup>), due to the proximity of residue 138 to the flavin in the FO conformation.

*What Is the Rate-Limiting Step in Turnover?* Regardless of the chemical nature of the step limiting the third phase of reduction, two lines of evidence suggest that no step in the reductive half-reaction is solely rate-limiting in turnover. First, since the slowest phase in the reductive half-reaction of wild-type thioredoxin reductase with NADPH at 25 °C is 53 s<sup>-1</sup>, and the steady-state turnover number at the same temperature is 33 s<sup>-1</sup>, it is evident that the reductive half-reaction is not solely rate-limiting. Second, the thermodynamic parameters determined from the temperature-dependent stopped-flow experiments are sufficiently different from those obtained from steady-state assays that it is not likely that they represent the same transition state(s). Thus, the conformational change may not be rate-limiting in catalysis by this enzyme. What does constitute the rate-limiting step will not be easy to determine. In previous work (Lennon & Williams, 1995), we proposed that in the absence of pyridine nucleotide no step in the oxidative half-reaction of thioredoxin reductase with thioredoxin was rate-limiting. It was only when pyridine nucleotide was present in the oxidative half-reaction that the observed rate constant for oxidation of the enzyme became slow enough to be rate-limiting. The proposal in that work was that the step which was limiting the oxidative half-reaction was either the conformational change proposed by Waksman et al. (1994) or dithiol/disulfide interchange between the active-site cysteines of the enzyme and the disulfide of thioredoxin. While the present work indicates that the conformational change is largely responsible for limiting the reductive half-reaction, dithiol-disulfide interchange may also be rate-limiting in turnover.

This study presents experimental data which indicate that the proposed conformational change is required in catalysis. The same experiments effectively eliminate two other

explanations for the third phase of the reductive half-reaction: dissociation of NADP<sup>+</sup> and reduction by a second equivalent of NADPH. Thus, it has been proposed that this phase results from the reduction of those enzyme molecules that exist in the FO conformation. We have also shown that the mutation of the active-site disulfide has significant effects on the reductive half-reaction of thioredoxin reductase, apart from any effects caused simply by the loss of the disulfide. It is possible that these effects result from the perturbation of the ratio of the FR and FO conformations present in the enzyme. Evidence obtained through fluorescence spectroscopy (Mulrooney & Williams, 1997) supports the suggestion that mutation in the active site can influence the ratio of the FR and FO conformations. It should be kept in mind that there has been no direct observation of the proposed conformational change, and so its association with the third phase of reduction must be treated as a working hypothesis. Strong support for these suggestions would be provided by a direct measure of the rate constant for the conformational change or by an independent measure of the FR/FO ratio in the various thioredoxin reductases studied. At present, we believe that the third phase of the reductive half-reaction of thioredoxin reductase to a large extent is limited by the conformational change between the FO conformation and the putative FR conformation.

## ACKNOWLEDGMENT

We thank Ms. Donna Veine for the creation, purification, and initial characterization of the TrxR(Ala<sup>135</sup>,Ala<sup>138</sup>) and TrxR(Ser<sup>135</sup>,Ser<sup>138</sup>) mutants, as well as the determination of the extinction coefficients of the active-site mutants of thioredoxin reductase. We thank Christopher M. Harris of Dr. Vincent Massey's laboratory in the Department of Biological Chemistry at The University of Michigan for sharing with us his mechanism and modeling results, which led to the mechanism and modeling shown in eq 2 and in the supporting information, Appendix A. We also thank Dr. David P. Ballou and Dr. Vincent Massey in the Department of Biological Chemistry at The University of Michigan for helpful discussions and Dr. John S. Blanchard in the Department of Biological Chemistry at the Albert Einstein College of Medicine of Yeshiva University for his critical reading of this manuscript.

## SUPPORTING INFORMATION AVAILABLE

Simulations of the mechanism shown in eq 2 and of a modification of Scheme 1 (12 pages). Ordering information is given on any current masthead page.

## REFERENCES

- Arscott, L. D., Gromer, S., Schirmer, R. H., Becker, K., & Williams, C. H., Jr. (1997) *Proc. Natl. Acad. Sci. U.S.A.* 94, 3621–3626.
- Beinert, H. (1960) in *The Enzymes*, 2nd Edition (Boyer, P. D., Lardy, H., & Myrback, K., Eds.) Vol. 2, pp 339–416, Academic Press, New York.
- Benen, J., van Berkel, W., Dieteren, N., Arscott, D., Williams, C., Jr., Veeger, C., & de Kok, A. (1992) *Eur. J. Biochem.* 207, 487–497.
- Blankenhorn, G. (1975) *Eur. J. Biochem.* 50, 351–356.
- Claiborne, A., & Ahmed, S. A. (1989) *J. Biol. Chem.* 264, 19864–19870.
- Fersht, A. (1985) in *Enzyme structure and mechanism*, 2nd ed., pp 140–141, W. H. Freeman and Company, New York.
- Holmgren, A. (1968) *Eur. J. Biochem.* 6, 475–484.

- Lennon, B. W., & Williams, C. H., Jr. (1995) *Biochemistry* 34, 3670–3677.
- Lennon, B. W., & Williams, C. H., Jr. (1996) *Biochemistry* 35, 4704–4712.
- Lennon, B. W., Ludwig, M. L., & Williams, C. H., Jr. (1997) *Protein Sci.* 6 (Suppl. 1), 107.
- Malcolm, A. D. B. (1980) *Methods Enzymol.* 66, 8–11.
- Massey, V., & Palmer, G. (1962) *J. Biol. Chem.* 237, 2347–2358.
- Massey, V., Matthews, R. G., Foust, G. P., Howell, L. G., Williams, C. H., Jr., Zanetti, G., & Ronchi, S. (1970) in *Pyridine Nucleotide-Dependent Dehydrogenases* (Sund, H., Ed.) pp 393–409, Springer-Verlag, Berlin.
- Moore, E. C., Reichard, P., & Thelander, L. (1964) *J. Biol. Chem.* 239, 3445–3452.
- Mulrooney, S. B., & Williams, C. H., Jr. (1994) *Biochemistry* 33, 3148–3154.
- Mulrooney, S. B., & Williams, C. H., Jr. (1997) *Protein Sci.* (in press).
- O'Donnell, M. E., & Williams, C. H., Jr. (1983) *J. Biol. Chem.* 258, 13795–13805.
- Palmer, G., & Massey, V. (1968) in *Biological Oxidations* (Singer, T. P., Ed.) pp 263–300, Interscience Publishers/John Wiley & Sons, New York.
- Prongay, A. J., & Williams, C. H., Jr. (1990) *J. Biol. Chem.* 265, 18968–18975.
- Prongay, A. J., & Williams, C. H., Jr. (1992) *J. Biol. Chem.* 267, 25181–25188.
- Prongay, A. J., Engelke, D. R., & Williams, C. H., Jr. (1989) *J. Biol. Chem.* 264, 2656–2664.
- Rietveld, P., Arscott, L. D., Berry, A., Scrutton, N. S., Deonarain, M. P., Perham, R. N., & Williams, C. H., Jr. (1994) *Biochemistry* 33, 13888–13895.
- Russel, M., & Model, P. (1988) *J. Biol. Chem.* 263, 9015–9019.
- Schopfer, L. M., Massey, V., Ghisla, S., & Thorpe, C. (1988) *Biochemistry* 27, 6599–6611.
- Segel, I. H. (1975) in *Enzyme Kinetics: Behavior and analysis of rapid equilibrium and steady-state systems*, pp 931–942, John Wiley & Sons, New York.
- Stoll, V. S., & Blanchard, J. S. (1990) *Methods Enzymol.* 182, 24–38.
- Strickland, S., Palmer, G., & Massey, V. (1975) *J. Biol. Chem.* 250, 4048–4052.
- Waksman, G., Krishna, T. S. R., Williams, C. H., Jr., & Kuriyan, J. (1994) *J. Mol. Biol.* 236, 800–816.
- Wang, P.-F., Veine, D. M., Ahn, S. H., & Williams, C. H., Jr. (1996) *Biochemistry* 35, 4812–4819.
- Williams, C. H., Jr. (1976) in *The Enzymes* (Boyer, P. D., Ed.) pp 89–173, Academic Press, New York.
- Williams, C. H., Jr. (1992) in *Chemistry and Biochemistry of Flavoenzymes* (Müller, F., Ed.) Vol. III, pp 121–211, CRC Press, Boca Raton, FL.
- Williams, C. H., Jr. (1995) *FASEB J.* 9, 1267–1276.
- Williams, C. H., Jr., Zanetti, G., Arscott, L. D., and McAllister, J. K. (1967) *J. Biol. Chem.* 242, 5226–5231.
- Williams, C. H., Jr., Prongay, A. J., Lennon, B. W., & Kuriyan, J. (1991) in *Flavins and Flavoproteins 1990* (Curti, B., Ronchi, S., & Zanetti, G., Eds.) pp 497–504, Walter de Gruyter & Co., Berlin.
- Zanetti, G., & Williams, C. H., Jr. (1967) *J. Biol. Chem.* 242, 5232–5236.
- Zanetti, G., Williams, C. H., Jr., & Massey, V. (1968) *J. Biol. Chem.* 243, 4013–4019.

BI970307J